E3S Web of Conferences **730**, 05015 (2026) https://doi.org/10.1051/e3sconf/202673005015
Soft Soils 2026

Settlement behaviour and watertightness evaluation of immersion joints in immersed tunnel on soft soil: a case study of the Noordtunnel

Prabendra A. Atmakusuma [1*], *Wout* Broere [2], *Harry R.E.* Dekker [3] and *Xuehui* Zhang [4]

[1] Directorate General of Highways, Ministry of Public Works, Jakarta, Indonesia
[2] Department of Geoscience and Engineering, Delft University of Technology, Delft, The Netherlands
[3] Rijkswaterstaat, Ministry van Infrastructure en Waterstaat, Utrecht, The Netherlands
[4] Department of Civil and Environmental Engineering, The Hong Kong Polytechnic University, Kowloon, Hong Kong, China

Abstract. Immersed tunnels are widely used to cross waterways and are typically constructed in deltaic regions where soft soil conditions prevail. Despite careful design, immersed tunnels founded on soft soil may experience excessive and differential settlements, which may lead to structural cracking or leakage during long-term operation. Understanding the settlement behaviour of immersed tunnels on soft soil therefore remains critical for ensuring tunnel structural safety and serviceability. This study investigates the settlement behaviour of the Noordtunnel, an immersed tunnel in the Netherlands that has been in operation for over three decades. Field settlement data were first compiled and analysed. Then, two-dimensional numerical models were developed using two soil constitutive models to simulate settlements from construction stage to long-term service conditions, including the effects of riverbed sedimentation above the tunnel roof. Model calibration and sensitivity analyses were conducted to verify predictive reliability. The findings indicate that the observed differential settlements are primarily attributed to the presence of soft subsoil layers and ongoing riverbed sedimentation. The implications of differential settlement for tunnel watertightness, particularly at immersion joints, are subsequently assessed.

1 Introduction

Tunnels and bridges are essential infrastructure solutions for crossing waterways, particularly in areas requiring high-capacity, uninterrupted transportation between geographically separated regions. For heavily trafficked waterways, tunnels are generally preferred because they do not interfere with maritime navigation. Among the various tunnel construction methods, immersed tunnels offer notable advantages due to their relatively shallow alignment beneath the water body, resulting in shorter tunnel lengths [1-2]. In addition, parallel execution of trench excavation and element fabrication reduces construction time and cost, while prefabrication typically results in fewer joints, lowering the potential risk of leakage [3]. As a result, immersed tunnels have become widely adopted in coastal and deltaic regions, where soft soil conditions frequently prevail. Since the early twentieth century, nearly 150 immersed tunnels for transportation purposes have been constructed worldwide [4]. Due to their length and alignment, immersed tunnels often traverse heterogeneous soil profiles, leading to non-uniform geotechnical conditions along the tunnel alignment [5].

Although the effective weight of immersed tunnel is generally lighter than the original soil it replaces, settlement may still be compelling and, in some cases, exceed the expected value derived from the geotechnical design [2]. Field evidence, such as the Kiltunnel in the Netherlands, demonstrates that settlement may result in structural cracking and leakage [6]. Differential settlement is of particular concern, as it may induce stress concentrations within the tunnel structure, leading to local cracking, damage to immersion joints, and potential leakage, which may shorten the tunnel's lifespan [7].

While numerous studies have focused on the construction phase and initial performance of immersed tunnels, comparatively limited attention has been given to long-term settlement behaviour and its effect on the risk of leakage. In this study, the settlement behaviour of an immersed tunnel and its impact on leakage risk are investigated using the Noordtunnel, an immersed road tunnel in the Netherlands, as a case study. The Noordtunnel has been in operation since 1990 and represents a typical immersed tunnel constructed on soft deltaic soil. Long-term monitoring has revealed pronounced differential settlement, particularly at a specific immersion joint, raising concerns regarding long-term serviceability and watertightness. Furthermore, reported leakages in the Noordtunnel have been documented in the SWECO [8] assessment. By integrating field settlement measurements with numerical modelling, this study aims to identify the

* Corresponding author: atmakusuma.ardhan@pu.go.id

governing mechanisms of differential settlement, predict future settlement, and assess the implications of settlement-induced joint deformation for tunnel watertightness.

2 Settlement and immersion joints of immersed tunnel

2.1 Settlement mechanisms of immersed tunnels on soft soil

Immersed tunnels constructed in deltaic and coastal environments are commonly founded on soft clay, peat, or organic deposits with low shear strength and high compressibility, making them susceptible to deformation. Settlement develops through a sequence of construction-induced stress changes: initial unloading during trench excavation, subsequent reloading from element placement and backfilling, followed by long-term consolidation and creep. Although the effective weight of an immersed tunnel is generally lower than that of the excavated soil—suggesting limited additional loading on the foundation—significant settlement may still develop and, in some cases, exceed values predicted during geotechnical design [2]. The magnitude of settlement is influenced by multiple factors, including ground conditions, design limitations, construction methods, and environmental influence [7].

From a structural perspective, uniform settlements are usually less of a concern than differential settlements. Uniform settlement corresponds to rigid-body displacement of the tunnel and typically does not induce structural damage. In contrast, differential settlement is commonly observed in immersed tunnels and is of greater concern, as it may cause relative rotation and deformation between adjacent tunnel elements, [9].

2.2 Immersion joints and watertightness considerations

An immersed tunnel is constructed from a series of prefabricated elements that are immersed and connected beneath the water surface. This segmented configuration gives rise to two types of joints during construction: immersion joints and dilation joints (Fig. 1(a)). Immersion joints are key structural components that connect two adjacent tunnel elements and ensure structural continuity and watertightness throughout the service life. These joints commonly consist of two components: the GINA gasket and the omega profile that rely on sufficient compressive force to maintain a watertight seal [10-11]. In addition, a cast-in-situ shear key is incorporated to provide vertical shear resistance, as illustrated in Fig. 1(b). Within a segmented tunnel element, dilation joints are formed as concrete-to-concrete interfaces, where sealing is achieved using embedded metal–rubber gaskets. Consequently, joint performance is sensitive to relative displacement, rotation, and deformation between tunnel elements.

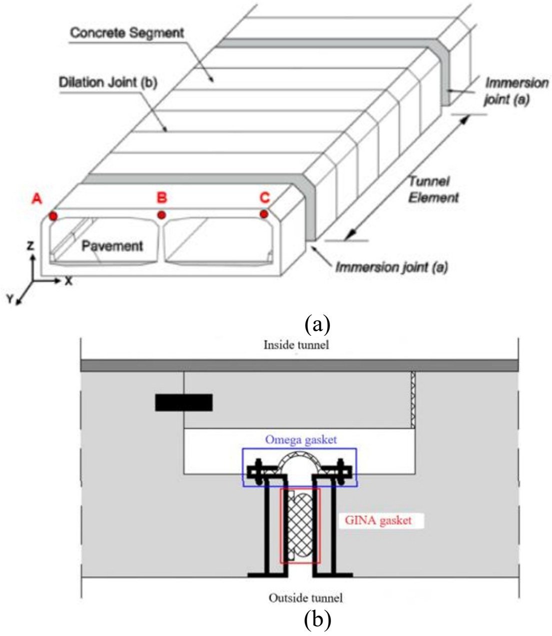

Fig. 1. The schematic of (a) segmented tunnel and (b) immersion joint [11].

Vertical deformation of immersed tunnels is primarily governed by differential settlement. Longitudinal non-uniform settlement may induce tilting of segment or elements and compression–decompression deformation at immersion joints. Decompression at the immersion joint causes a joint opening, affecting the rubber sealing performance and raising a watertightness issue. Meanwhile, joint compression causes a joint closure that could lead to overcompression of the joint [11]. Although leakage is reported to occur more frequently at dilation joints [12], this study focuses exclusively on immersion joints due to limited availability of monitoring data.

Leakage at immersion joints is commonly associated with degradation or failure of the GINA and Omega seals [13]. As the Omega seal is not designed to resist direct compression and serves as a secondary sealing system, this study adopts a conservative approach by evaluating leakage risk based on the compression–decompression behaviour of the GINA gasket.

During construction, the tunnel element is immersed and linked to other finished ones on the riverbed or the approach structure. The GINA gasket, positioned on one end of the element, undergoes compression due to the water pressure. The extent of compression depends on the depth of the element immersed in water. The initial compression of the GINA gasket is determined from the force-compression curve of the GINA type used.

Differential settlement induces relative rotation between adjacent tunnel elements, which may lead to compression or decompression at the immersion joint. Accordingly, joint deformation is evaluated based on the geometric relationship, rotation centre, and tilting angle of the elements. The resulting joint opening or closure is derived from the rotation-induced displacement at the gasket location.

Watertightness is evaluated by examining the force equilibrium between the frictional resistance of the rubber gasket and the external loads acting on it [13], as illustrated in Fig. 2. The frictional resistance (Fr) is computed as the product of the gasket compression force and the rubber–steel friction coefficient. In this case, a friction coefficient of 0.6 is selected. This equilibrium represents a worst-case scenario in which bolt resistance is neglected due to full corrosion.

$$F_r \geq F_w + F_g \quad (1)$$

where F_r represents the friction force of the rubber gasket to the two sides of steel plates, while F_w and F_g are the upstream water pressure force and soil cover force, respectively.

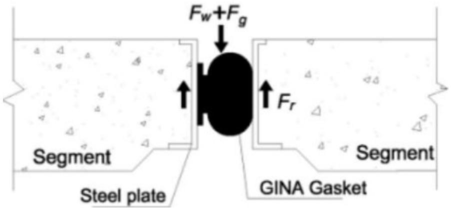

Fig. 2. The visualization of frictional resistance (*Fr*) and external load acting on GINA gasket [11].

In this study, time-dependent relaxation of the GINA gasket is accounted for using an empirical reduction factor. A relaxation coefficient of 5% per decade (*r*) is adopted, following standard Trelleborg design value [13], with the time duration (*t*) calculated in years post-immersion. Thus, the remaining force percentage can be estimated using the subsequent formula.

$$R = 1 - 0.01 \cdot r \cdot \log(t \cdot 365 \cdot 24 \cdot 60) \quad (2)$$

Moreover, determining the external force applied to the rubber gasket involves an initial calculation of the joint width, which represents the rubber gasket's surface area subjected to the external force. The joint width is determined by subtracting the compression value induced by differential settlement from the initial height of the GINA gasket.

$$Rh_i = h_0 - \Delta h \quad (3)$$

where ho is the uncompressed height of the GINA gasket and Δh is the calculated compression width.

3 Settlement analysis of the Noordtunnel

3.1 Overview of the Noordtunnel and Geological Condition

The Noordtunnel is a bidirectional road tunnel connecting Alblasserdam to Hendrik-Ido Ambacht in South Holland. The tunnel passes beneath the Noord River and was constructed between 1988 and 1991, with the immersion phase completed within approximately three months (October–December 1990). The tunnel accommodates six traffic lanes (three in each direction) and includes a central emergency escape corridor that separates the traffic directions and enhances safety during emergency conditions.

The immersed section of the Noordtunnel consists of four prefabricated tunnel elements with a total length of approximately 430 m. Each element is subdivided into several shorter structural segments during prefabrication in the dry dock to facilitate construction and handling. A typical tunnel cross-section is approximately 31.95 m wide and 8.02 m high, while the length of an individual immersed segment is approximately 21.2 m, as shown in Fig. 3.

The subsoil profile along the tunnel alignment is generally uniform, consisting of a soft upper layer of clay and peat, underlain by a sand layer, and a ±10 m thick clay stratum, which overlies deeper sandy deposits (Fig. 4).

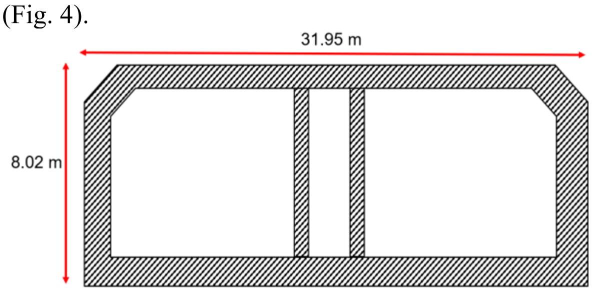

Fig. 3. Schematic cross-sectional view of the Noordtunnel.

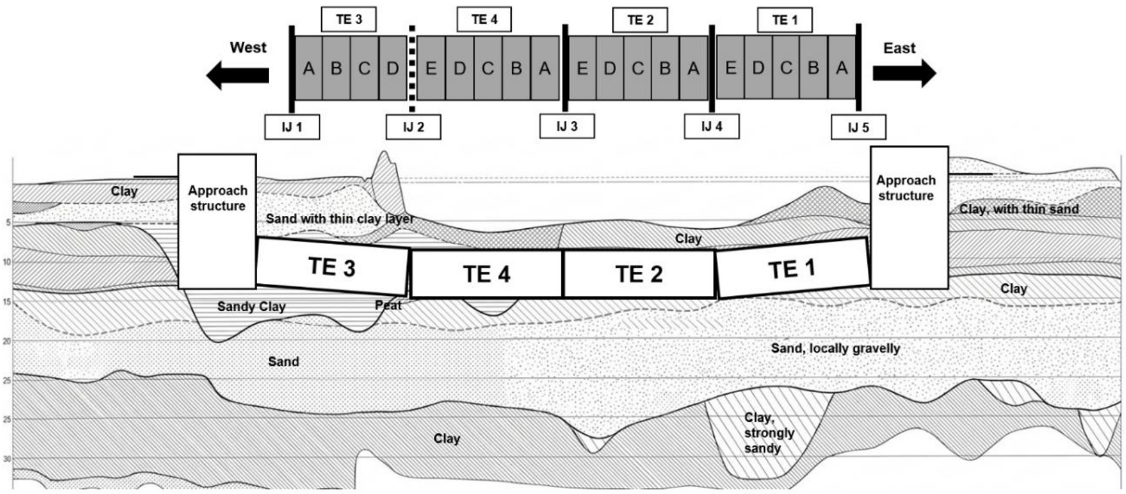

Fig. 4. Schematic longitudinal tunnel and subsoil stratigraphy (not to scale).

3.2 Settlement monitoring data

The settlement of the Noordtunnel were measured during two distinct periods: the first ten months following immersion and long-term monitoring from 1993 to 2019. Due to gaps and incompleteness in the records, settlement magnitudes during unmeasured periods were estimated by interpolating the trendline of available data. Taking immersion joint 2 as an example, Fig. 5 shows that the initial measurement recorded relatively large settlements—mainly due to primary consolidation. After approximately 206 days, the rate of settlement noticeably declined, and the trendlines began to flatten, indicating the onset of secondary compression (creep).

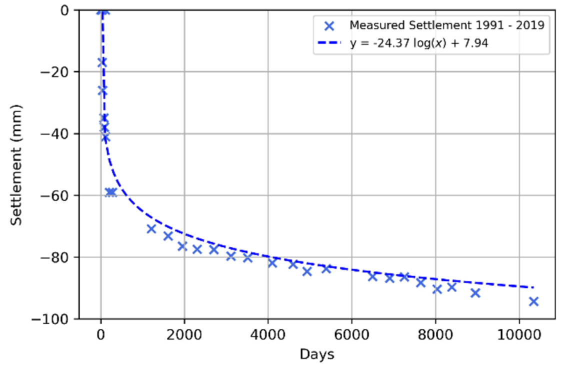

Fig. 5. The post-immersion measured settlement at immersion joint 2.

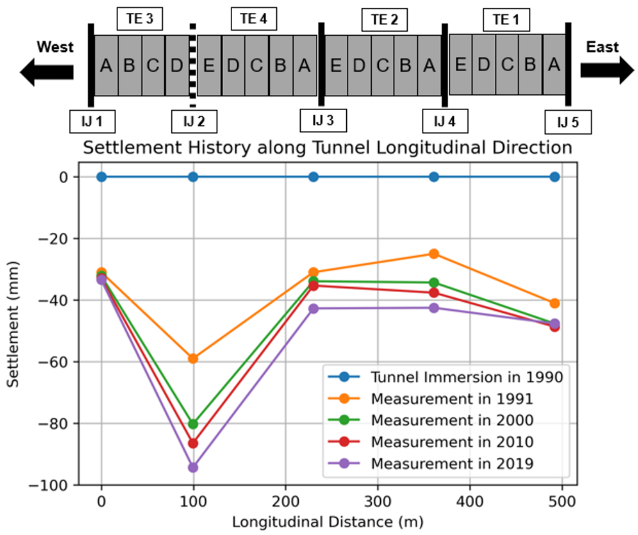

Fig. 6. Settlement history along tunnel longitudinal direction.

The settlement tendencies at the other immersion joints are determined by applying the same approach. As depicted in Fig. 6, it is observed that uneven settlement along the tunnel's longitudinal axis, with Immersion Joint 2 (IJ2) showing a significantly higher total settlement of 94.36 mm by 2019, compared to 33–48 mm at other joints.

3.3 Model description

The numerical modelling aims to analyse the settlement behaviour of the Noordtunnel and predict its long-term performance. As settlement measurements are available at discrete immersion joints, the tunnel is represented by five independent two-dimensional transverse cross-sectional models, each corresponding to a specific immersion joint location. This approach enables direct comparison with field measurements while accounting for local variations in subsoil conditions. This modelling strategy was adopted as longitudinal 2D modelling of the tunnel would require artificial assumptions, such as modifying concrete properties to prevent uplift and defining the properties of in-plane direction as non-porous, which may suppress pore pressure development. In addition, the maximum gradient between adjacent tunnel elements is approximately 4%, indicating limited longitudinal interaction effects. Therefore, the adopted cross-sectional modelling approach is considered adequate to provide a consistent and representative description of soil–structure interaction and soil behaviour at specific locations. In this paper, Immersion Joints 2 and 3 are presented as representative examples for the development and application of the two-dimensional model.

The 2D finite element models were developed in PLAXIS based on as-built drawings, incorporating detailed tunnel geometry and material properties as described in Section 3.1. To minimise boundary effects, the model domain was set to 250 m in width and 75 m in depth, consistent with recommended practice (i.e. 3–5 times the tunnel dimensions), as shown in Fig. 7.

Settlement was simulated over the full construction and operational sequence, including trench dredging, installation of a 0.5 m sandflow foundation, tunnel immersion, backfilling, ballast application, and long-term sedimentation. The trench base was set at 14.751 m below NAP, with side slopes beginning 4 m from the tunnel base at a 1:4 inclination and a height of 10.251 m. Excavation induce subsoil unloading and rebound, followed by reloading due to element placement and backfilling. Additional sedimentation at immersion joint 2 is also being considered by adding 1.5 m clay layer above the tunnel.

Given the unloading–reloading sequence and the presence of soft compressible soils, the Hardening Soil (HS) model is adopted to simulate short-term behaviour, while the Soft Soil Creep (SSC) model is used to capture long-term deformation and time-dependent settlement effects. The soil parameters were derived from laboratory test and CPT-based correlations in accordance with NEN guidelines, and are summarised in Tables 1 and 2, respectively. The parameter set indicates low stiffness and high compressibility for the soft clay and peat layers, and relatively higher stiffness for sandy strata.

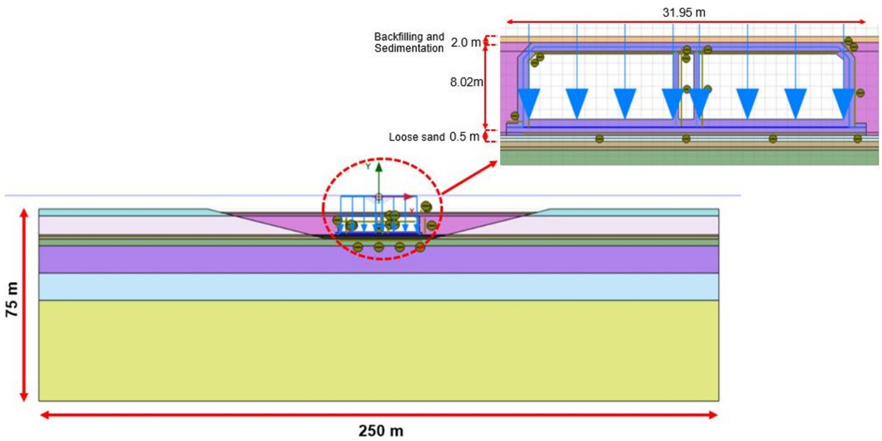

Fig. 7. The numerical model – soil domain.

Table 1. The subsoil properties at Immersion Joint 2.

Soil Type	Thickness (m)	γ_{sat} (kN/m^3)	c (kN/m^2)	ϕ (°)	HS Soil Parameters			SSC Soil Parameters		
					$E_{50}{}^{ref}$ (MPa)	$E_{oed}{}^{ref}$ (MPa)	$E_{ur}{}^{ref}$ (MPa)	λ^*	μ^*	κ^*
Sandy clay	2.5	16	5	22	2	1	6	0.067	0.002	0.044
Sand (often silty with thin clay)	7.5	16	5.4	21.6	5	5	15	-	-	-
Base Peat	1	12	5	28	1	0.5	3	0.100	0.003	0.067
Sand (fine to medium)	12.5	20	0	35	32.43	32.43	97.31	-	-	-
Clay (often sandy or silty)	10	20	13	22.5	6	3	18	0.031	0.001	0.021
Sand (fine and silty)	37	21	0	35	16.87	16.87	50.62	-	-	-

Table 2. The subsoil properties at Immersion Joint 3.

Soil Type	Thickness (m)	γ_{sat} (kN/m^3)	c (kN/m^2)	ϕ (°)	HS Soil Parameters			SSC Soil Parameters		
					$E_{50}{}^{ref}$ (MPa)	$E_{oed}{}^{ref}$ (MPa)	$E_{ur}{}^{ref}$ (MPa)	λ^*	μ^*	κ^*
Peat	3	11	5	25	0.5	0.25	1.5	0.133	0.004	0.089
Clay (with plant remains)	4.5	14	7	20	1	0.5	3	0.100	0.003	0.067
Base Peat	1	12	5	28	1	0.5	3	0.100	0.003	0.067
Sand (fine to medium)	16.5	20	0	35	33.82	33.82	101.5	-	-	-
Clay (often sandy or silty)	8	20	13	22.5	5	2.5	15	0.033	0.001	0.023
Sand (fine and silty)	37	21	0	35	16.87	16.87	50.62	-	-	-

3.4 Settlement result analysis

The simulations results are compared to the monitoring data for validation and to figure out the settlement tendency of the immersion joints. Fig. 8 presents the settlement trendlines in the HS and SSC models (indicated in red and green trendlines, respectively) alongside the monitoring data. Both models show similar settlement tendencies during the initial 206 days, indicating primary compression occurred in the first seven months. Minor differences in settlement magnitude during this period are attributed to variations in the yield surfaces of the two constitutive models.

After seven months of immersion, the HS model predicts negligible additional settlement, as no further loading is applied and excess pore water pressures have fully dissipated. In contrast, the SSC model continues to exhibit gradual settlement due to creep effects. The monitored settlement data (shown in blue) generally display a flattening trend consistent with the HS model response, except at Immersion Joint 2. This phenomenon is highly likely due to the presence of localized peat and clay underneath the second immersion joint. Soft soil typically has high compressibility, making them susceptible to volume reduction and settlement under applied loads. Consequently, creep behaviour becomes prominent in the second immersion joint, leading to ongoing settlement after the primary compression stage. Quantitatively, approximately 20 mm of settlement is attributed to the soft subsoil beneath the tunnel segment, while an additional 8 mm is associated with ongoing natural sedimentation.

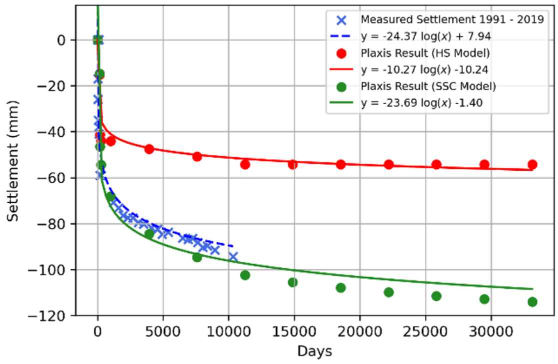

(a)

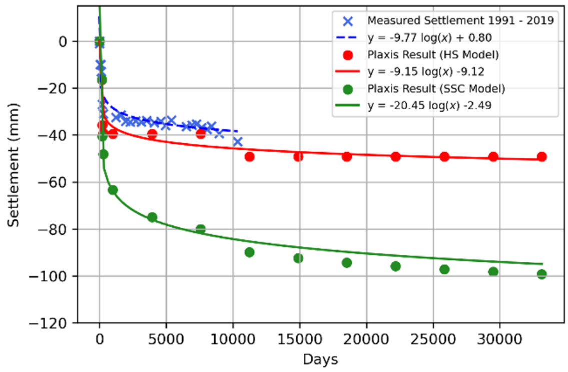

(b)

Fig. 8. The simulation results at (a) immersion joint 2 and (b) immersion joint 3 (which represents the settlement trend at immersion joints 1, 4, and 5).

3.5 Settlement prediction

The model is calibrated using the sensitivity analysis, with a main objective of quantifying potential deviations from its initial result. The analysis starts by pinpointing the soil layers contributing most significantly to settlement. The soil stiffness parameter values are tried to be set by using Python to randomize a set of parameter values based on the normal distribution model. Afterwards, the confidence interval (5th and 95th percentile) of the data was selected to determine how much settlement would deviate from its initial results due to stiffness variability in the field.

The results indicate that the stiffness parameters E_{oe}d and E_{ur} are negatively correlated with settlement, such that higher stiffness values lead to reduced deformation. In contrast, the creep parameters (μ*) shows a positive correlation, with higher values resulting in increased settlement. Due to the relatively narrow range of stiffness values observed in the field, varying E_{ur} within 90% of its distribution produces only minor settlement deviations (0.3–2.0 mm) at immersion joints 1, 3, 4, and 5. However, adopting the lower-bound stiffness (p5) increases settlement by approximately 1.3–1.5 mm. At immersion joint 2, adjusting μ* to the upper and lower bounds of its reference distribution results in settlement changes of +1.9 mm and −5.55 mm, respectively.

As illustrated in Fig. 9, the sensitivity analysis demonstrates the deviations remains below 4% across most immersion joints, reaching a maximum of 5.48% at joint 2. These results validate the model's robustness and its suitable for projecting future settlement trends.

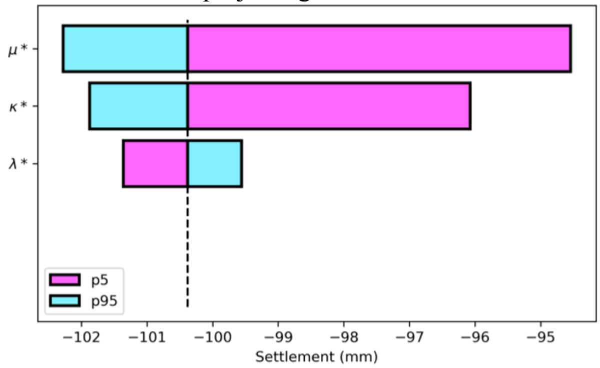

(a)

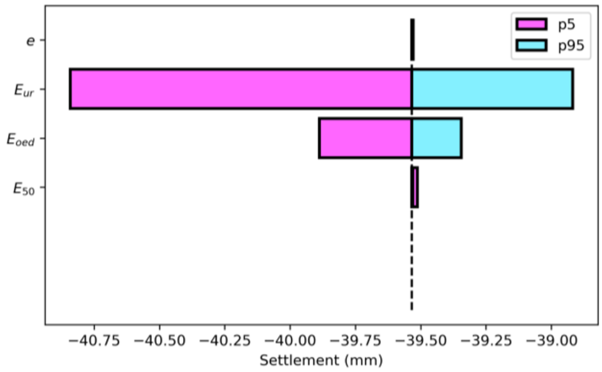

(b)

Fig. 9. The sensitivity analysis result for (a) clay at IJ 2 and (b) sand at IJ 3 (which represents the sensitivity analysis trend at immersion joints 1, 4, and 5).

The forthcoming settlement of the Noordtunnel is estimated by identifying the settlement tendency that closely matches the monitoring data. The Soft Soil Creep (SSC) model is applied at immersion joint 2, where soft soil layers are present, while the Hardening Soil (HS) model is used for the remaining joints. According to the modelling results, the settlement tends to flatten at immersion joint 1,3,4, and 5. This suggests that the pore water pressure can dissipate in a relatively short time period. Additionally, only the second immersion joint shows a slightly larger settlement rate for the upcoming years due to the creep effect caused by soft soil in the subgrade. Projections indicate that immersion joint 2 will experience approximately 15.13 mm of additional settlement by the end of the tunnel's designed service life. In contrast, joints 1, 3, 4, and 5 are expected to undergo 4–5 mm of further settlement over the next 67 years. These estimates are detailed in Table 3 and visualized in Fig. 10.

Table 3. The settlement prediction.

Years	Settlement (mm)				
	IJ 1	IJ 2	IJ 3	IJ 4	IJ 5
2024	-37.20	-98.39	-46.58	-49.23	-54.19
2030	-37.67	-100.06	-47.23	-49.93	-54.87
2040	-38.33	-102.36	-48.11	-50.89	-55.81
2060	-39.32	-105.82	-49.45	-52.34	-57.22
2090	-40.36	-109.49	-50.87	-53.88	-58.72

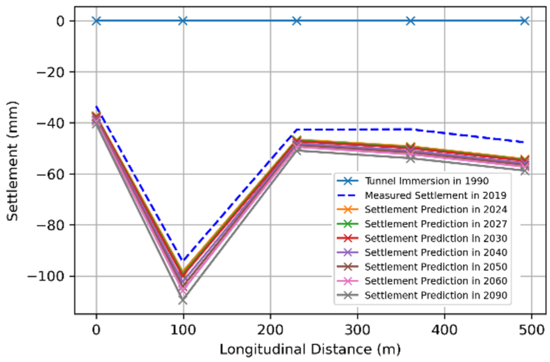

Fig. 10. Longitudinal settlement prediction along tunnel alignment.

3.6 Watertightness evaluation

As previously described in Section 2.2, the non-uniform settlement has the potential to induce longitudinal tilting of tunnel elements, resulting in unequal compression or decompression of the immersion joints. The illustration presented in Fig. 11 depicts the inclination of tunnel elements resulting from the differential settlements, indicated in red dashed lines. The tilting center of the tunnel elements is set to be at the tunnel floor of each tunnel element with less settlement. The positive sign indicates compression, while the negative sign represents decompression in immersion joints. It can be observed that decompression occurs at the roof of immersion joints 1, 3, 5 and at the floor of immersion joints 2 and 4. Meanwhile, the compression occurs at the roof of immersion joints 2 and 4. Decompression at the immersion joint causes a joint opening, affecting the rubber sealing performance and raising a watertightness issue.

The joint opening and closure at each immersion joints are quantified based on the displacement induced by relative rotation of adjacent tunnel elements, as described in Section 2.2. However, it should be noted that the second immersion joint is a closure joint where a rigid joint is used at that particular location instead of a flexible joint. Therefore, immersion joint 2 is not considered in the calculation.

Table 4. The calculated and predicted joint opening/closure.

Years	Location	IJ 1	IJ 2	IJ 3	IJ 4	IJ 5
2019	Roof (mm)	-6.07	-	-1.94	1.89	-1.91
	Floor (mm)	0	-	-0.40	-0.15	0
2040	Roof (mm)	-6.52	-	-1.74	1.92	-2.20
	Floor (mm)	0	-	0	-0.13	0
2090	Roof (mm)	-6.99	-	-1.96	2.01	-2.31
	Floor (mm)	0	-	0	-0.13	0

To examine the potential risk of leakage at the immersion joints, it is necessary to determine the initial compression of the GINA gasket. The magnitude of compression is governed by the immersion depth of the tunnel element and the force–compression relationship of the specific GINA type employed. In the Noordtunnel, GINA type ETS-130-160 is used at all immersion joints. Table 5 summarises the calculated hydrostatic pressures and corresponding initial gasket compressions for each joint. The initial compression of the GINA is set as the baseline condition, and the remaining gasket compression for each assessment year is obtained by superimposing the calculated joint opening or closure (Table 4) onto this baseline value.

The watertightness of immersion joints is evaluated by assessing the equilibrium between the frictional resistance of the rubber gasket and the external loads acting on the GINA gasket. Leakage is assumed to occur when the combined water and soil pressures exceed the available frictional resistance. Equations (1) – (3) are therefore employed to assess joint watertightness.

Table 5. The calculated and predicted joint opening/closure.

Description	IJ 1	IJ 2	IJ 3	IJ 4	IJ 5
Depth (section-middle, m)	10.24	-	10.24	12.31	11.07
Hydrostatic force (kN)	25800	-	25800	30760	27801
GINA gasket length (m)	75.23	-	75.23	75.23	75.23
Force per meter (kN/m)	342.97	-	342.97	408.90	369.56
Initial compression (mm)	69	-	69	72	70.5

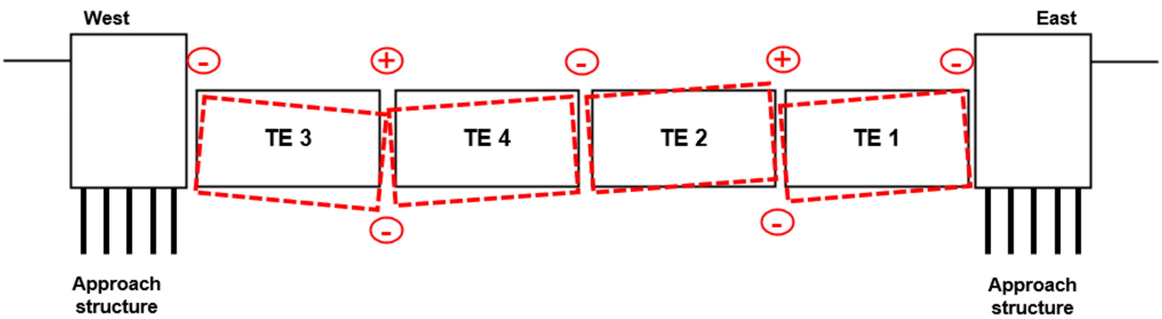

Fig. 11. The illustration of longitudinal compression and decompression at immersion joints (not to scale).

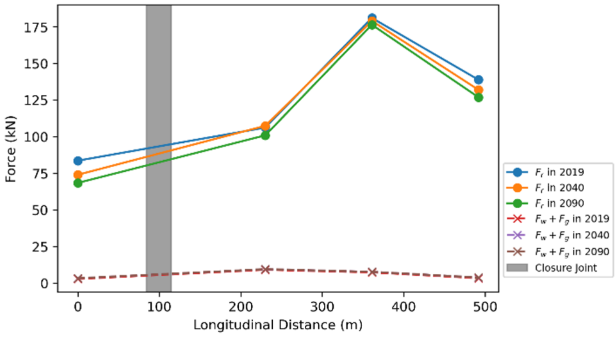

Fig. 12. Comparison of friction force against external force at the tunnel roof over time.

It can be observed from Fig. 12 that the external pressures applied on the GINA gasket, illustrated with dashed lines, are significantly lower in magnitude compared to the total friction force. It shows that the impact of uneven settlement on the water tightness of immersion joints is generally minimal.

4 Conclusion

This study investigated the long-term settlement behaviour of an immersed tunnel constructed on soft deltaic soil and evaluated its implications for joint watertightness, using the Noordtunnel in the Netherlands as a case study. Based on the combined analysis of field monitoring data and two-dimensional numerical modelling, the following conclusions can be drawn:

1. Field measurements indicate that the majority of tunnel settlement occurred within the first seven months after immersion, corresponding to primary consolidation. Thereafter, settlement rates decreased significantly, with secondary compression governing long-term behaviour.
2. Pronounced differential settlement was observed along the tunnel alignment, with Immersion Joint 2 experiencing larger settlement than other joints. This behaviour is mainly attributed to the presence of soft soil layers beneath the tunnel segment, combined with ongoing natural sedimentation above the tunnel roof.
3. Numerical simulations using the Hardening Soil (HS) and Soft Soil Creep (SSC) models successfully reproduced the measured settlement trends. While the HS model adequately captured short-term settlement, the SSC model was essential for representing long-term, time-dependent deformation in soft soils.
4. Sensitivity analysis indicates that settlement is strongly influenced by soil stiffness and creep parameters. Given the narrow distribution of the reference values, variation of the most sensitive parameters results in a maximum deviation of 5.48% at Immersion Joint 2 and less than 4% at the remaining joints, demonstrating that the model is sufficiently robust for long-term settlement prediction.
5. Long-term projections suggest an additional settlement of approximately 15.1 mm at Immersion Joint 2 over the next 67 years, whereas only 4–5 mm of further settlement is expected at the remaining immersion joints.
6. Differential settlement induces relative rotation and compression–decompression of immersion joints. However, watertightness assessment indicates that the frictional resistance of the GINA gasket remains sufficient to maintain watertightness under the predicted settlement conditions.

References

1. A. Glerum, Immersed tunnels: why, when, and where, Tunneling and Underground Space Technology, 3:347–351, (1988)
2. T.T. K. Olsen and J. de Wit, Immersed tunnel in soft soil conditions experience from the last 20 years, Tunneling and Underground Space Technology, (2022)
3. R. Lunnis and J. Baber, Immersed Tunnel, CRC Press, (2023)
4. Q. Ouyang, C. Qi, S. Sun, B. Yan, W. Pan, Y. Huang, and J. Ma, Experimental Study on the Dynamic Response of an Immersed Tunnel Element Moored Inside The Harbor, MDPI, Marinde Science and Engineering, Vol. **13**, Issue 14 https://doi.org/10.3390/app13148456
5. Z. Hu, Y. Xie, and J. Wang, Challenges and strategies involved in designing and constructing a 6 km immersed tunnel: A case study of the Hong Kong–Zhuhai–Macao Bridge, Tunneling and Underground Space Technology, **50**: 171–177, (2015)
6. K. Gavin, W. Broere, M.S. Kovačević, and K. de Haas, Investigation of the remaining life of an immersed tube tunnel in the Netherlands. In D. Peila, G. Viggiani, & T. Celestino (Eds.), Tunnels and Underground Cities: Engineering and Innovation Meet Archaeology, Architecture and Art (pp. 4831–4838), CRC Press, (2019)
7. W.C. Grantz, Immersed tunnel settlements part 1: Nature of settlements. Tunneling and Underground Space Technology, **16**:195–201, (2001)
8. SWECO, North Tunnel risk analysis. SWECO Netherlands BV, Bilt, (2020)
9. X. Zhang and W. Broere, Settlements of immersed tunnel on soft ground: A case study. Tunnels and Underground Cities: Engineering and Innovation meet Archaeology, Architecture and Art, pages 1234–124, (2019)
10. ITA, Guideline for Immersed Tunnels, International Tunnelling Association, (2010)
11. X. Zhang and W. Broere, Monitoring seasonal deformation behavior of an immersed tunnel with distributed optical fiber sensors. Measurement, 219, (2023)
12. L. Leeuw, Lekkage in tunnels II, COB, (2018)
13. R. van Montfort, Insufficiency of immersion joints in existing immersed tunnels. Case study on functioning of Gina-seal and Omega-seal in the Kil Tunnel. Master's thesis, Delft University of Technology, (2018)